Quantum dynamics in high-spin molecules, spin dendrimers, and spin lattices

ARTICLE *in* INTERNATIONAL JOURNAL OF QUANTUM CHEMISTRY · DECEMBER 2005

Impact Factor: 1.43 · DOI: 10.1002/qua.20801

Quantum Dynamics in High-Spin Molecules, Spin Dendrimers, and Spin Lattices

MASAHIRO TAKAHATA,[1] MITSUO SHOJI,[1] HIROYA NITTA,[1] RYO TAKEDA,[1] SHUSUKE YAMANAKA,[1] MITSUTAKA OKUMURA,[1] MASAYOSHI NAKANO,[2] KIZASHI YAMAGUCHI[1]

[1]*Department of Chemistry, Graduate School of Science, Osaka University, Machikaneyama 1-1, Toyonaka, Osaka 560-0043, Japan*

[2]*Department of Materials Engineering Science, Graduate School of Engineering Science, Osaka University, Toyonaka, Osaka 560-8531, Japan*

Received 6 March 2005; accepted 14 July 2005
Published online 6 September 2005 in Wiley InterScience (www.interscience.wiley.com).
DOI 10.1002/qua.20801

ABSTRACT: We perform spin dynamics in strongly correlated electron–spin systems to clarify the relationship between the phase relaxation and the structure of the spin systems. The interaction among spins is considered to be Heisenberg-type exchange. The quantum Liouville approach is used for the dynamics involving the relaxation processes of the systems, which is considered to originate in spin–phonon and electron spin–nuclear spin interactions. As a first step of our study, to examine the effects of the structures on the phase relaxation, we consider the phenomenological relaxation parameters for the relaxation terms of quantum Liouville equation, and perform the spin dynamics in four types of four electron–spin systems that have linear, square, star (dendritic structure), and tetrahedral structures. The results of our calculation indicated the possibility for the control of the phase relaxation by the change of the structure in spin clusters. Possible implications of our results are related to the single-molecule magnets, ESR-STM detection of spins, and related spin-transition phenomena (decoherence and population relaxation). Int J Quantum Chem 105: 615–627, 2005

Key words: spin dynamics; Liouville equation; spin–phonon interaction; Glauber magnet; quantum memory; ESR-STM

Correspondence to: M. Takahata; e-mail: mtaka@chem.sci.osaka-u.ac.jp

Contract grant sponsor: Japan Society for the Promotion of Science (JSPS).

Contract grant numbers: 14204061; 14340184.

1. Introduction

In biological systems, there are many sophisticated features, which are still inimitable by artificial devices and chemical syntheses [1–5]. For example, there are several materials involved in the living bodies, e.g., proteins, and several mechanisms, e.g., energy conversion in the photosynthesis, information processing of brain and sensors for the five senses. In particular, photosynthesis is known to have an efficient mechanism as energy-harvesting function. Moreover, several dendrimers are synthesized as the artificial imitations for the materials [6]. The dendrimers are known to have several unique architectures, and to have some interesting properties, which are related to their architectures. Several theoretical studies [7–9] clarified that the relaxation mechanism plays an important role for such an energy transfer in one direction. In general, relaxation is energy dissipation processes with the destroy of the coherent phase. In particular, the proteins are considered the origin of the relaxation because they construct the soft environment of biological system. The consideration of relaxation process becomes more important as the size of the system is larger. There is a possibility of the control of relaxations in a number of biological systems such as the enzymatic reactions, electron transfer reactions, and energy harvesting [1–5].

We have studied the excitation energy transfer in aggregate systems considering exciton migration originated in exciton–phonon interaction [7–9]. In our previous study [10] we have extended the theory to spin dynamics involving spin–phonon interactions that play important roles in several types of molecular magnetism; (1) photo-induced magnetic transition, (2) high-spin (HS) to low-spin (LS) transitions induced by pressure, etc., (3) single molecular magnet (SMM), (4) ESR-STM detection of single spin, and (5) quantum computation by electron spins. The magnetic dendrimers have been considered as an example of SMM with very slow relaxation [10].

As a continuation of previous work, the relaxation processes in the spin dynamics are focused in this study. We perform spin dynamics in strongly correlated electron–spin systems in order to clarify the relation between the phase relaxation and the structures of spin clusters. The interaction among spins is considered to be Heisenberg-type exchange. Quantum Liouville approach is used for the dynamics involving the relaxation processes of the systems. At the first step of our study, we consider the phenomenological relaxation parameters for the relaxation terms of the quantum Liouville equation. At first, we consider the two electron–spin system [11], which is the simplest model with one interaction. Next, we study several four electron–spin systems, which have peculiar architectures, e.g., linear, square, star (dendritic structure), and tetrahedral structures, in order to examine the relations between the phase (coherence) relaxation and the structures of the spins. Possible implications of our results for the relations between magnetisms and aggregate structures are related to the ESR-STM detection of spins, and related spin-transition phenomena (decoherence and population relaxation).

2. Theoretical Background

2.1. THREE VARIABLES FOR THE MAGNETIC PROPERTIES

In this section we briefly summarize key concepts and theoretical results for the present work, since the size effects in molecular magnets are not systematically discussed yet. As discussed previously [12, 13], in magnetism, three important variables should be taken into account: (a) spin dimensionality, (b) magnetic lattice dimensionality (1D, 2D, and 3D), and (c) scale factor (microscopic, mesoscopic, and macroscopic). The magnetic properties (M) can be regarded as functions of three variables: $M = f(\mathrm{a}, \mathrm{b}, \mathrm{c})$, as illustrated in Figure 1. These properties of molecule-based materials are generally described by the following spin Hamiltonian:

$$\hat{H}_{\mathrm{general}} = \hat{H}_{\mathrm{XY}} + \hat{H}_{\mathrm{I}}, \tag{1}$$

where $\hat{H}_{\mathrm{XY}}$ and $\hat{H}_{\mathrm{I}}$ are the XY and Ising Hamiltonians defined by

$$\hat{H}_{\mathrm{XY}} = -2J_{\mathrm{XY}} \sum (S_i^x S_{i+1}^x + S_i^y S_{i+1}^y), \tag{2a}$$

$$\hat{H}_{\mathrm{I}} = -2J_{\mathrm{Z}} \sum S_i^z S_{i+1}^z. \tag{2b}$$

The Heisenberg model is a special case in Eq. (1): $J_{\mathrm{XY}} = J_{\mathrm{Z}} = J_{\mathrm{HB}}$.

$$\hat{H}_{\mathrm{HB}} = -2J_{\mathrm{HB}} \sum S_i \cdot S_j. \tag{3}$$

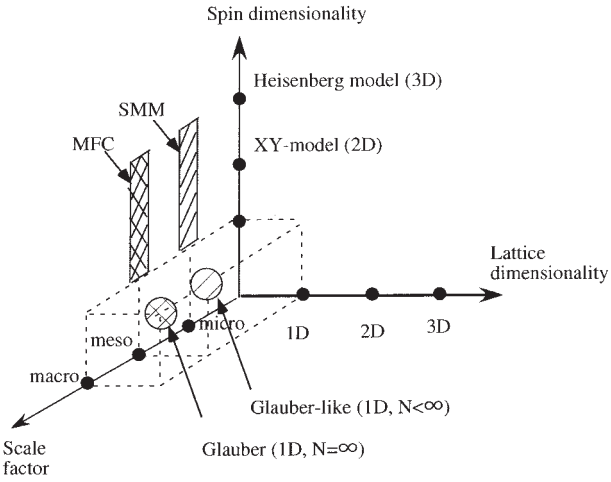

FIGURE 1. Magnetic properties of molecule-based magnets as a function of three variables; SMM (single moleculed magnets) and MFC (mesoscopic ferromagnetic cluster).

In past decades, the typical three-dimensional case (a = HB, b = 3D, and c = macroscopic) has been attracted for design and synthesis of molecule-based magnets with higher critical temperatures [14]. Pure organic bulk ferro-, antiferro-, and ferrimagnets have been realized by crystallization of nitroxide radicals with different molecular structures [14].

Recently low-dimensional magnetic materials have been actively investigated in relation to the so-called nanoscience. For example, single-molecule magnets (SMM), microscopic in scale factor and zero-dimension (0D) in lattice dimension [15–20], have been interesting targets both experimentally and theoretically as shown in Figure 1. Mesoscopic ferromagnetic clusters (MFC), such as $(M)_N$ (M = Fe, Co, Ni; N = 10–600), have been generated by the laser evapolation technique and their magnetic properties are elucidated by the Stern–Gerlach experiments [21–23]. Now, 1D-Ising magnets, Glauber magnets (GM) [24–33], are attracting renewed interest due to their slow relaxation of magnetization, though the long-range order cannot be expected for GM. Similarly, the 2D-Heisenberg magnets do not exhibit the long-range order. The addition of the anisotropic term (DS_z^2) to them is also an interesting attempt to accomplish slow relaxation of the magnetization. Figure 1 is useful and handy for understanding of future directions in the field of molecule-based magnets [12, 13].

2.2. SLOW RELAXATION OF 1D-ISING SPIN SYSTEM

The 1D-Ising Hamiltonian in Eq. (2b) is rewritten in the Glauber form [24] as

$$\hat{H}_G = -J \sum \sigma_i \sigma_{i+1}, \qquad (\sigma_i = \pm 1), \qquad (2c)$$

where J is given by $2J_z S_i S_{i+1}$, assuming that $S_i^z = S_i \sigma_i$ and $S_{i+1}^z = S_{i+1}\sigma_{i+1}$, and where S_k ($k = i, i+1$) denotes the size of Ising spin. Here, the N-site ring is considered as a model of the 1D-Ising chain as illustrated in Figure 2. The partition function of the ring is well-known as

$$Z = \sum_{\sigma_1} \sum_{\sigma_2} \cdots \sum_{\sigma_N} \exp\left(\frac{J}{kT} \sum \sigma_i \sigma_{i+1}\right) = \left[2\cosh\left(\frac{J}{kT}\right)\right]^N. \qquad (N \gg 1), \quad (4)$$

where k is the Boltzmann constant. The Gibbs free energy is then easily derived as

$$G = -NkT \ln\left[2\cosh\left(\frac{J}{kT}\right)\right]. \qquad (5)$$

The nearest-neighbor spin correlation function $\tau(T)$, magnetic specific heat C_M, and magnetic susceptibility χ are derived from G as follows:

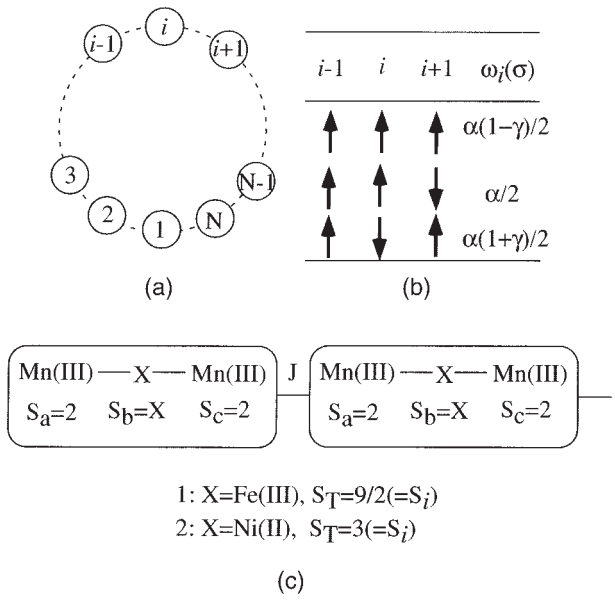

FIGURE 2. N-site ring (a) and Glauber magnets.

$$\tau(T) = \langle \sigma_i \sigma_{i+1} \rangle = \tanh\left(\frac{J}{kT}\right), \tag{6a}$$

$$C_M = \frac{NJ^2}{kT^2} \cosh^2\left(\frac{J}{kT}\right), \tag{6b}$$

$$\chi(T) = \frac{N}{kT} \exp\left(\frac{2J}{kT}\right). \tag{6c}$$

Continuous functions of T exhibit no anomaly in conformity, with no phase transition in the 1D-Ising infinite chain.

However, the short-range spin correlation $\langle \sigma_i \sigma_{i+1} \rangle$ may be responsible for the relaxation process of magnetization. Glauber has performed theoretical studies of this slow relaxation process, using the master equation approach [24]:

$$\frac{d}{dt} P(\sigma_1, \sigma_2, \cdots \sigma_N; t) = -\left[\sum_i \omega_i(\sigma_i)\right] P(\sigma_1, \sigma_2, \cdots \sigma_N; t) + \sum_i \omega_i(-\sigma_i) P(\sigma_1, \sigma_2, \cdots, -\sigma_i, \cdots \sigma_N; t), \tag{7}$$

where P denotes the probability function of N-spin ring with the $\sigma_1, \sigma_2, \cdots \sigma_N$ spin configuration, and $\omega_i(\pm\sigma_i)$ means the probability per unit time that the ith spin flips from the value $\sigma_i(-\sigma_i)$ to $-\sigma_i(\sigma_i)$ while the others remain fixed. The probability including the alignment effect of the nearest-neighbor spins may be written as

$$\omega_i(\sigma_i) = \frac{\alpha}{2}\left\{1 - \frac{1}{2}\gamma\sigma_i(\sigma_{i-1} + \sigma_{i+1})\right\}, \tag{8}$$

where α is the inverse of the relaxation constant (τ). Three possible values of $\omega_i(\sigma_i)$ are feasible depending on spin alignments as illustrated in Figure 2. The parallel (antiparallel) configurations will be long-lived than the antiparallel (parallel) ones as long as γ is positive (negative). The equilibrium condition of spin population requires that $P_i(\pm\sigma_i)$ should be expressed by the Boltzmann statistics, giving rise to the explicit expression of $\gamma = \tanh(2J/kT)$.

To investigate the relaxation process, Glauber [24] examined the 1D Ising chain under the time-dependent magnetic field H

$$\hat{H} = -J \sum \sigma_i \sigma_{i+1} - H \sum \sigma_i. \tag{9}$$

The detailed balancing (near-equilibrium) condition is assumed for $P_i(\pm\sigma_i)$ and $\omega_i(\pm\sigma_i)$ as

$$\frac{P_i(-\sigma_i)}{P_i(\sigma_i)} = \frac{\omega_i(\sigma_i)}{\omega_i(-\sigma_i)} \frac{[1 - \sigma_i\beta]}{[1 + \sigma_i\beta]}, \tag{10}$$

where $\beta = \tanh(H/kT)$. The magnetization constructed by all spins is defined using the stochastic function $\sigma_i(t)$ as

$$M(t) = \sum_k \sigma_k(t). \tag{11a}$$

The expectation value of the magnetization is easily derived under the assumption of the harmonic magnetic field, $H(t) = H_0 e^{-i\omega t}$, as

$$\langle M(t) \rangle = \chi(\omega) H_0 e^{i\omega t}. \tag{11b}$$

The magnetic susceptibility $\chi(\omega)$ is expressed by the real and imaginary parts:

$$\chi(\omega) = \chi'(\omega) + i\chi''(\omega), \tag{12a}$$

where

$$\chi'(\omega) = \chi(T) \frac{\alpha^2(1-\gamma)^2}{\alpha^2(1-\gamma)^2 + \omega^2}, \tag{12b}$$

$$\chi''(\omega) = \chi(T) \frac{\alpha^2(1-\gamma)\omega}{\alpha^2(1-\gamma)^2 + \omega^2}. \tag{12c}$$

Then, if $J \gg kT$, $\chi''(\omega)$ should be observed and the relaxation time ($\tau = \alpha^{-1}$) depends exponentially on the temperature. The relaxation process is also dependent on the magnitude of the effective exchange integral (J).

Very recently, Glauber magnets have been realized by several research groups [30–33], and the relaxation times of the magnetization and other magnetic properties have been elucidated by the high-field ESR experiments. For example, Yamashita's group [31–33] have shown that the trimer unit [Mn(III)—X—Mn(III)][X=Fe(III), Ni(II)] forms the 1D-Ising chain [Eq. (2b)] or 1D general chain [Eq. (1)] with small ferromagnetic exchange coupling constant $J > 0$, as shown in Figure 2. Their results also indicated an important role of both J and anisotropic term ($D_i S_i^2$) for activation barrier of spin inversion. From a theoretical view point, ab initio

computation [34–36] of J_{ij} and D_i is very important for the rational design of single-molecule magnets with high transition temperatures.

2.3. MAGNETIC BEHAVIORS OF CLUSTER MAGNETS

In this section, let us consider microscopic and mesoscopic magnetic clusters (b = 0D and c = micro or meso) in Figure 1. The magnetization of a single spin M under the magnetic field H is given by the thermal average of its M_z component ($J, J-1, \ldots, -J$) as

$$\langle m \rangle = \sum M_z \exp\left(-\frac{M_z H}{kT}\right) \Big/ \sum \exp\left(-\frac{M_z H}{kT}\right) = JB_J\left(\frac{JH}{kT}\right), \quad (13a)$$

where $B_J(x)$ denotes the Brillouin function. The $B_J(x)$ function has been used to describe variation of the magnetization of component spin for molecule-based magnets. The magnetic moment of ferromagnetic cluster $(M)_N$ is given by $N \times J$. If JN is quite large, the giant magnetic moment can be regarded as a classical spin, whose magnetization is given by

$$M_N = JNL\left(\frac{JNH}{kT}\right) \cong \frac{J^2N^2H}{kT}, \quad (13b)$$

where $L(x)$ is the Langevin function:

$$L(x) = \coth x - \frac{1}{x} [\equiv B(x), J \to \infty]. \quad (14)$$

The $L(x)$ function becomes $x/3$ if $x \ll 1$. The magnetization per atom in the cluster is therefore expressed by

$$m_N = \frac{M_N}{N} = \frac{J^2}{3k}\left(\frac{NH}{T}\right). \quad (13c)$$

This means that the m_N value for small cluster is scaled by the cluster size; $H/T \times N$ [21]. The size dependence of m_N has been really observed in the Co cluster ($N \cong 50$–150) [21]. This, in turn, implies that cluster spin (JN) can be regarded as classical in nature. The crossover from quantum to classical spin should occur at $N < 50$.

However, the giant spin of transition metal clusters $(M)_N$ (M = Fe, Co, Ni; N = 50–150) remains superparamagnetic. It was found that the giant spin really exhibits a pseudo-phase transition (PPT) when N exceeds about 500 in the case of the $(Ni)_N$ cluster. Here, PPT is different from the thermodynamic phase transition (TPT) of bulk transition metal ($N = \infty$). For example, the magnetic moment of $(M)_N$ ($N \cong 500$) is not zero, even over the transition temperature (T_0) of PPT [22, 23]. The T_0-value for PPT is lower than the T_c of TPT as

$$T_0 = T_C - \text{const} \times (N)^{-1/3}. \quad (15)$$

For example, T_0 is 350 K for $(Ni)_N$ (N = 230), although T_c = 625 K ($N = \infty$) [23].

The bulk metal of 4d transition elements (M = Rh, Ru, Pd, . . .) is nonmagnetic in nature, although single atom (M) is paramagnetic. Therefore, clusters of these atoms $(M)_N$ should exhibit a PPT from superparamagnetic to the nonmagnetic state. In fact, such a transition has been found in the cases of $(Rh)_N$ and $(Ru)_N$ clusters, and the critical numbers (N*) for PPT are about 60 and 20, respectively [37, 38]. From a theoretical view point, the unrestricted hybrid DFT (HDFT) solutions of the $(M)_N$ cluster should reduce to the restricted HDFT solutions. The development of order-N method is desirable for reliable first-principle computations of mesoscopic clusters in this regards [39, 40].

2.4. QUANTUM BEHAVIORS OF CLUSTER SPINS

The quantum behaviors of spin clusters are increasingly important when cluster sizes become smaller and smaller [41]. Three different cases are conceivable for variations of magnetic properties of quantum spins: (a) (de)coherence of quantum phase (ϕ) of spins in the single state $|S, m\rangle$, (b) transitions between spin multiplet states of electron spins; $|S, m\rangle \leftrightarrow |S, m \pm i\rangle$ (i = 1, 2, . . .), and (c) spin crossover between different spin states; $|S, m\rangle \leftrightarrow |S', m'\rangle$ ($S \neq S'$). Figure 3 illustrates three cases (a, b, c) for molecular quantum spins.

The (de)coherence [Fig. 3(a)] of the quantum phase of small spin clusters is of current interest in relation to quantum computation [42–44] and the quantum information transfer [45]. The quantum control of coherent motion of spins by quantum light is an important and interesting problem for these purposes. Nakano and Takahata and colleagues [7–9, 46–48] have developed several simulation methods of quantum phase dynamics of excitons (pseudo spins) interacting with coherent and

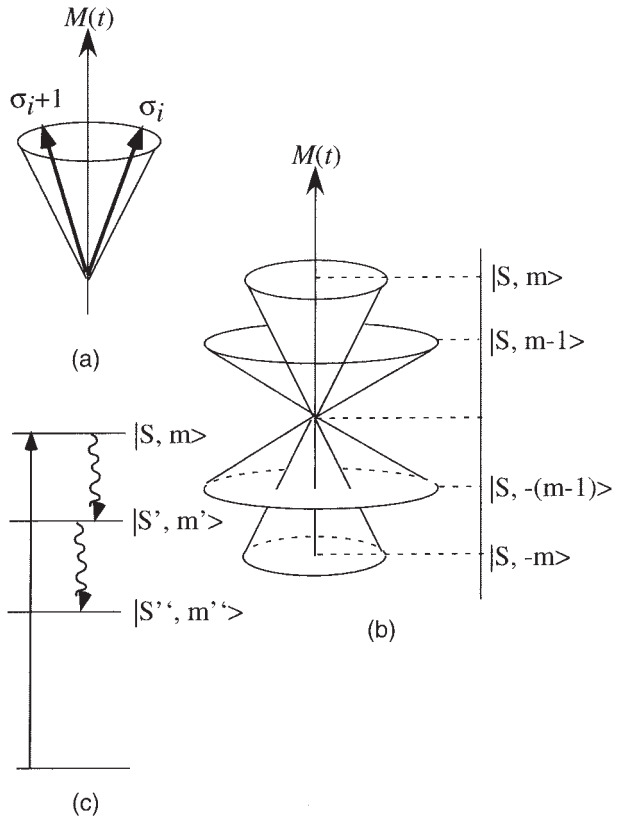

FIGURE 3. Spin transitions, (a) dephasing, (b) spin tunneling, and (c) spin crossover.

squeezed quantum lights. Their methods can be applicable to any spin–boson systems in general. Then the spin–boson model has been extended to elucidate common pictures of quantum spins, excitons, Bose–Einstein condensation (BEC), and BCS superconductivity [49–55].

The quantum spin tunneling problem in Figure 3(b) becomes increasingly serious when the size of magnetic memory becomes small. During the past decade, many theoretical and experimental studies were carried out for single molecule magnets (SMM), such as the Mn_{12}–A_c complex [15–19]. Nagao, Nishino, and Shigeta and their colleagues [56–58] have developed several analytical and computational methods for the investigation of the quantum effects of SMM: (i) coherent state path integral (PI) representation of the nonlinear σ-model [56, 58], (ii) numerical computation of the time-dependent Schrödinger equation [59], and (iii) ab initio path integral Monte Carlo (PIMC) method [56, 60].

The coherent PI method has been applied to elucidate tunneling probability of manganese oxide clusters with triangular, butterfly, and tetrahedral structures; triangular and Kagome lattices; 1D antiferromagnetic ring; and some clusters of clusters. Here, the potential curves for these species are expressed by the simplest double-well potential:

$$E = \langle H_{\text{eff}} \rangle = -a \cos^2\theta + b, \tag{16}$$

where two wells are expressed by $\theta = 0$ and π, and activation barrier is given by a. The parameters a and b are functions of J_{ij} and D_i: $a = f(J_{ij}, D_i)$ and $b = g(J_{ij}, D_i)$. The tunneling probability is generally given by

$$p \cong (\tau)^{-1} = ca \exp\left(-\frac{a}{2}\right), \tag{17}$$

where c is the topological factor given by $\cos(\pi S)$. Therefore, the c-value is 1 for integer spin ($S = 1, 2, \ldots$) but zero for half-integer spin ($S = 1/2, 3/2, \ldots$). This selection rule is often broken because of other magnetic interactions such as the hyperfine interactions between electron spin (S) and nuclear spin (I) [61–63]. Unfortunately, the blocking temperature is very low (<2K) at the present stage [13–17], showing further improvements. The rational design of molecular and cluster structures are thus crucial to raise the activation barrier (a) for quantum tunneling.

The spin crossover phenomena displayed in Figure 3(c) have been attracted in relation to magnetic field-induced transition (MFIT) in the transition-metal wheel compounds such as $(Fe)_6$ and $(Cu)_6$ [64, 65], and the light-induced excited spin trapping (LIESST) transitions of certain iron(II) complexes [66]. The coherent path integral (PI) formulation by the use of natural orbitals of ab initio UHF and UHDFT solutions has been performed for MFIT [60]. The Monte Carlo (MC) technique has been used to perform effective numerical simulations based on this formulation. The PIMC combined with the order-N ab initio calculations will be used instead of the Heisenberg model Hamiltonian in future [57]. The spin–phonon interaction has been found to be very important in the LIESST phenomena [66] and single molecule magnet [67–71] (it is studied in detail in Section 3).

2.5. AB INITIO CALCULATIONS OF ANISOTROPIC MAGNETIC INTERACTION TERMS

From the above discussion, ab initio calculations of isotropic (J_{ij}) and anisotropic magnetic interac-

tion terms are desirable for the rational design of 1D Glauber magnets [24–33], SMM [15–20], and other molecule-based magnets [14]. The ab initio computational procedures of J_{ij} have been developed extensively [34, 35]. Several relaxation processes are determined by anisotropic terms as follows:

(1) Second-order one-center term [36]:

$$\hat{H}_{\mathrm{ani}}(1) = \sum_i \left[D_i \left\{ (S_i^z)^2 - \frac{1}{3} S(S+1) \right\} + E_i \{ (S_i^x)^2 - (S_i^y)^2 \} \right], \quad (18)$$

(2) Two-center magnetic dipole–dipole [72] interaction term (D_{ij}) arising from

$$\hat{H}_{\mathrm{ani}}(2) = -\frac{1}{2} g^2 \mu_B \times \sum_{i,j} \left[\frac{3(\boldsymbol{S}_i \cdot \boldsymbol{r}_{ij})(\boldsymbol{S}_j \cdot \boldsymbol{r}_{ij}) - \boldsymbol{r}_{ij}^2 \boldsymbol{S}_i \cdot \boldsymbol{S}_j}{\boldsymbol{r}_{ij}^5} \right], \quad (19)$$

(3) Dzyalosinski–Moriya term [73]:

$$\hat{H}_{\mathrm{ani}}(3) = \sum_{i,j} \boldsymbol{d}_{ij} \cdot [\boldsymbol{S}_i \times \boldsymbol{S}_j], \quad (20)$$

(4) Hyperfine and electron spin–nuclear spin interactions [61–63]:

$$\hat{H}_{SI} = \hat{H}_{\mathrm{ani}}(4a) = -\sum_{i,j} a_{ij} \boldsymbol{S}_i \cdot \boldsymbol{I}_j, \quad (21a)$$

$$\hat{H}_{\mathrm{ani}}(4b) = -\frac{1}{2} g^2 \mu_B \times \sum_{i,j} \left[\frac{3(\boldsymbol{S}_i \cdot \boldsymbol{r}_{ij})(\boldsymbol{I}_j \cdot \boldsymbol{r}_{ij}) - \boldsymbol{r}_{ij}^2 \boldsymbol{S}_i \cdot \boldsymbol{I}_j}{\boldsymbol{r}_{ij}^5} \right], \quad (21b)$$

(5) Fourth-order term [74]:

$$\hat{H}_{\mathrm{ani}}(5) = \sum_i C_i \{ (S_i^+)^4 + (S_i^-)^4 \}, \quad (22)$$

(6) Spin–phonon coupling terms [67–71].

The spin–orbit and spin–other orbit interactions and main origins of the anisotropic terms (1), (3), and (5).

$$\hat{H}_{\mathrm{SO}} = g\mu_B^2 \sum_i \frac{Z_n \boldsymbol{S}_i \cdot \boldsymbol{M}_{ni}}{\boldsymbol{r}_{ni}^3} - \sum_{i,j} \frac{2\boldsymbol{S}_i \cdot \boldsymbol{M}_{ij} + \boldsymbol{S}_i \cdot \boldsymbol{M}_{ji}}{\boldsymbol{r}_{ij}^3}. \quad (23)$$

We have already developed our own programs to calculate D_i, E_i, D_{ij}, and d_{ij} terms by the ab initio procedures [35, 72, 73]. The c-value in Eq. (21) is usually too small to be determined by the ab initio calculations at the present stage [74]. There are several explicit expressions of spin–phonon coupling (H_{SP}) in the case of the Mn_{12}–A_c complex [67–71]. It has been shown that the spin–phonon coupling, together with D_i and C_i, play important roles of spin tunneling process in the system. However, the spin dynamics simulations, including all the terms (1)–(6), are too complex for the Mn_{12}–A_c complex [69]. In the next section, the spin–phonon coupling effects are examined phenomenologically in relation to the relaxation processes of molecular spins.

3. Computational Method and Procedure

In Section 2, we examined molecule-based magnetism in terms of scale factor in Figure 1. The raise of activation barriers in SMM and Glauber magnets are necessary for realization of quantum spin memories in future. From both theoretical and experimental backgrounds, one of the most challenging problems is the manipulation of electron spin by quantum light [75–77], electron current [78] and other techniques. Very recently, the ESR-STM technique has attracted great interest in relation to detection of single spin [79–82]. The development of such technique may prompt a realization of quantum computing by electron spin [83]. From this expectation, we have formulated spin–phonon (boson) interactions in the Markov approximation in order to investigate spin dynamics of molecular magnets with fractal architectures. As a continuation of previous work [10], we have further examined the relaxation processes of electron spin via spin–phonon interaction and electron spin–nuclear spin interaction [Eq. (21)]. Here, at the first step of this spin dynamics, these interactions are treated phenomenologically.

Our computational procedure is shown in Figure 4. We consider the spin aggregate interacted by the isotropic interactions, which is given by the spin Hamiltonian:

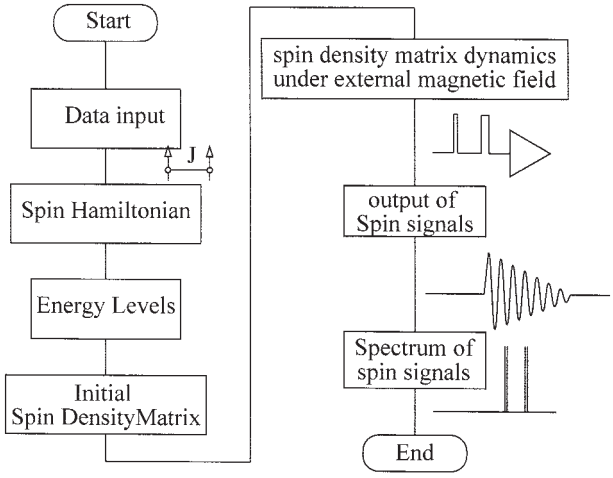

FIGURE 4. Flowchart of our calculation procedure.

$$\hat{H}(t) = -\sum_{\langle i,j\rangle} 2J_{ij}\hat{S}_i \cdot \hat{S}_j + \mu \sum_{i}^{N} g_i H(t)\hat{S}_i, \qquad (24)$$

where S_i is the spin operator of the spin i, and the summation is carried out over neighboring spin sites. The first term represents Heisenberg-type exchange interactions between spins. The second term is the interactions between spins and external magnetic field. The anisotropic magnetic interactions are negligibly small compared with isotropic interaction, especially in the case of spin dynamics at room temperature.

For the diagonalization of the Hamiltonian, we use the basis which constructed from a direct product of a state vector for each spin $\{|\varphi_{i_k}^k\rangle\}$:

$$|\varphi_{i_1}^1\varphi_{i_2}^2 \cdots \varphi_{i_N}^N\rangle \equiv |\varphi_{i_1}^1\rangle \otimes |\varphi_{i_2}^2\rangle \otimes \cdots \otimes |\varphi_{i_N}^N\rangle, \qquad (25)$$

where i_k represents a state for each spin:

$$|\varphi_1^k\rangle \equiv |\alpha^k\rangle, \qquad \text{(up spin)} \qquad (26)$$

$$|\varphi_2^k\rangle = |\beta^k\rangle, \qquad \text{(down spin)}. \qquad (27)$$

By diagonalizing the Hamiltonian H, we obtain new states with eigenenergies $\{E_n\}$ and eigenstates $\{|n\rangle\}$;

$$H|n\rangle = E_n|n\rangle. \qquad (28)$$

The time development for the spin model is performed by the quantum Liouville equation:

$$i\hbar \frac{\partial}{\partial t}\rho(t) = [\hat{H}(t), \rho(t)] - i\hat{\Gamma}\rho(t), \qquad (29)$$

where the second term represents the relaxation terms in the Markov approximation:

$$\{-\Gamma\rho(t)\}_{mn} = \begin{cases} -\Gamma_{mm}\rho_{mm} + \sum_{l\neq m}^{N} \gamma_{lm}\rho_{ll}, & (m = n), \\ -\Gamma_{mn}\rho_{mn}. & (m \neq n). \end{cases} \qquad (30)$$

The time development is calculated using the fourth-order Runge–Kutta method. The diagonal and off-diagonal parts are population and coherence relaxations, respectively. These terms are related to the T_1 and T_2 values in the magnetic resonance. These relaxation matrices are represented as follows:

$$\Gamma_{mn} = \begin{cases} \sum_{l\neq m}^{N} \gamma_{ml}, & (m = n), \\ \frac{1}{2}(\Gamma_{mm} + \Gamma_{nn}) + \Gamma'_{mn}, & (m \neq n), \end{cases} \qquad (31)$$

where Γ'_{mn} is pure coherence relaxation term. Because the spin dynamics to thermally stable state is performed, the relaxation coefficient γ is assumed to be

$$\gamma_{mn} = C \exp\left(-\frac{E_n - E_m}{2kT}\right). \qquad (32)$$

C is the relaxation parameter, which is related to the speed of the dynamics. This expression is used for the realization of the Boltzmann distribution in the thermally equilibrium:

$$\rho_{nn}(t = \infty) = \frac{\exp(-E_n/kT)}{\sum_s^N \exp(-E_s/kT)}. \qquad (33)$$

In a liquid, this relaxation is due to the fluctuation of local magnetic field from magnetic dipoles and electronic current by molecular rotations. Such effects originated in spin–lattice relaxations and spin–spin relaxations are taken into account for the physical origin of the phenomenological relaxation term in Eqs. (30) and (31).

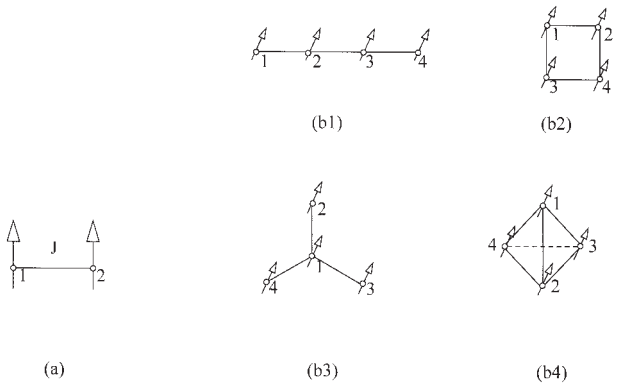

FIGURE 5. Structures of several spin clusters: simplest two-spin model (a) and four types of four-spin model: (b1) linear, (b2) square, (b3) star (dendritic), and (b4) tetrahedron. The interaction between spins are represented by a connected line.

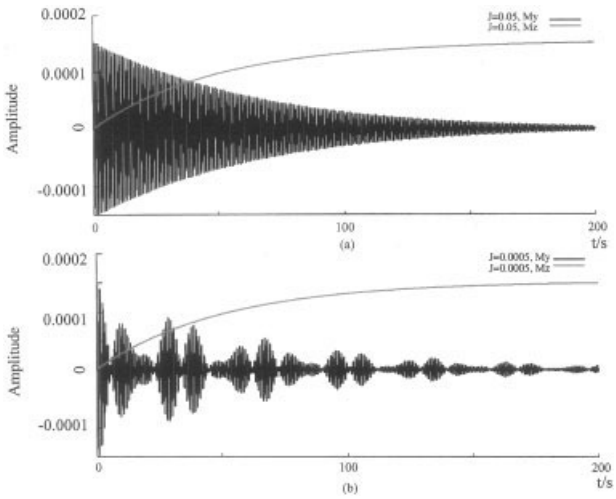

FIGURE 6. Variation of spin population (*Mz*) and coherency (*My*) for the two-spin model with the strong (a) and weak (b) interactions.

4. Results and Discussion

4.1. TWO-SPIN SYSTEM

Figure 5(a) shows the two spin model as a simplest spin cluster. This model has four spin states [one singlet state ($S = 0$: $m = 0$) and three triplet spin states ($S = 1$: $m = 1, 0, -1$)]. For the ferromagnetic material, for which the J-value is positive ($J > 0$), the excitation energy of the triplet states is lower than that of the singlet state. For the spin dynamics, we consider two situations, $J < B$ ($J = 0.0005\ \text{cm}^{-1}$) and $J > B$ ($J = 0.05\ \text{cm}^{-1}$), where one is the weak-interaction case and the other is strong one. To distinguish between two sites, g-values are assumed to be $g1 = 1.0$ and $g2 = 0.9$ in both simulations. The relaxation parameter is fixed at $C = 0.005$. External temperature and static magnetic field are fixed to be $T = 300$ K and $Bz = 23.5$ T, respectively. Figure 6 shows the variations of spin population for each case. In both cases, *Mz* values become initial populations in the thermally equilibrium with almost the same time. These processes are called population relaxations. The intensities of *My* values are found to decrease oscillating periodically. These processes are called phase relaxation. In this study, we do not show the result of *Mx* values because they have only rectangle phase for *My* signals. As the intensity of J becomes larger ($J > B$), *Mz* and *My* are found to be the same spin signals as that in Figure 6(b).

Figure 7(a) shows the schematic energy levels of two spin system with the interaction $J > 0$ on external magnetic fields. In this system, the spin state $|S = 0: m = -1\rangle$ has higher excitation energy than state $|S = 0: m = 1\rangle$ has. After the first excitation by rotational magnetic field, the spin state $|S = 0: m = -1\rangle$ has a small population, and then the relaxations between triplet spin states occur. The FFT spectrum has only one singlet signal (not shown in this paper). In the other case of a small J value ($J < B$), the *My* signal is convoluted. The FFT spectrum has two doublet signals at the $g1$ and $g2$ shift positions. The split of the signals is equal to the value of the J interaction. Spin signals are obtained by the use of multifrequency coherent magnetic radiation in the microwave and radiofrequency range pro-

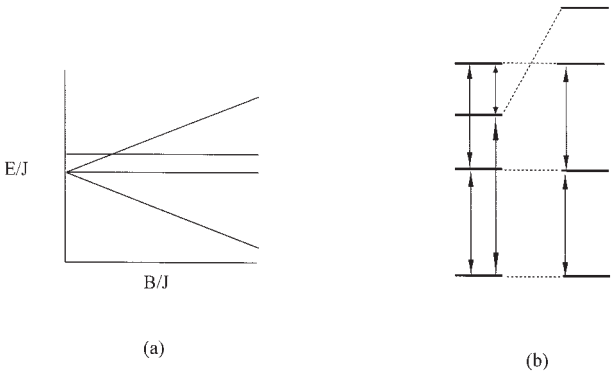

FIGURE 7. Schematic energy level of two spin model as a function of external magnetic field (a) and in the two cases (b) $B > J$ (right) and $J > B$ (left).

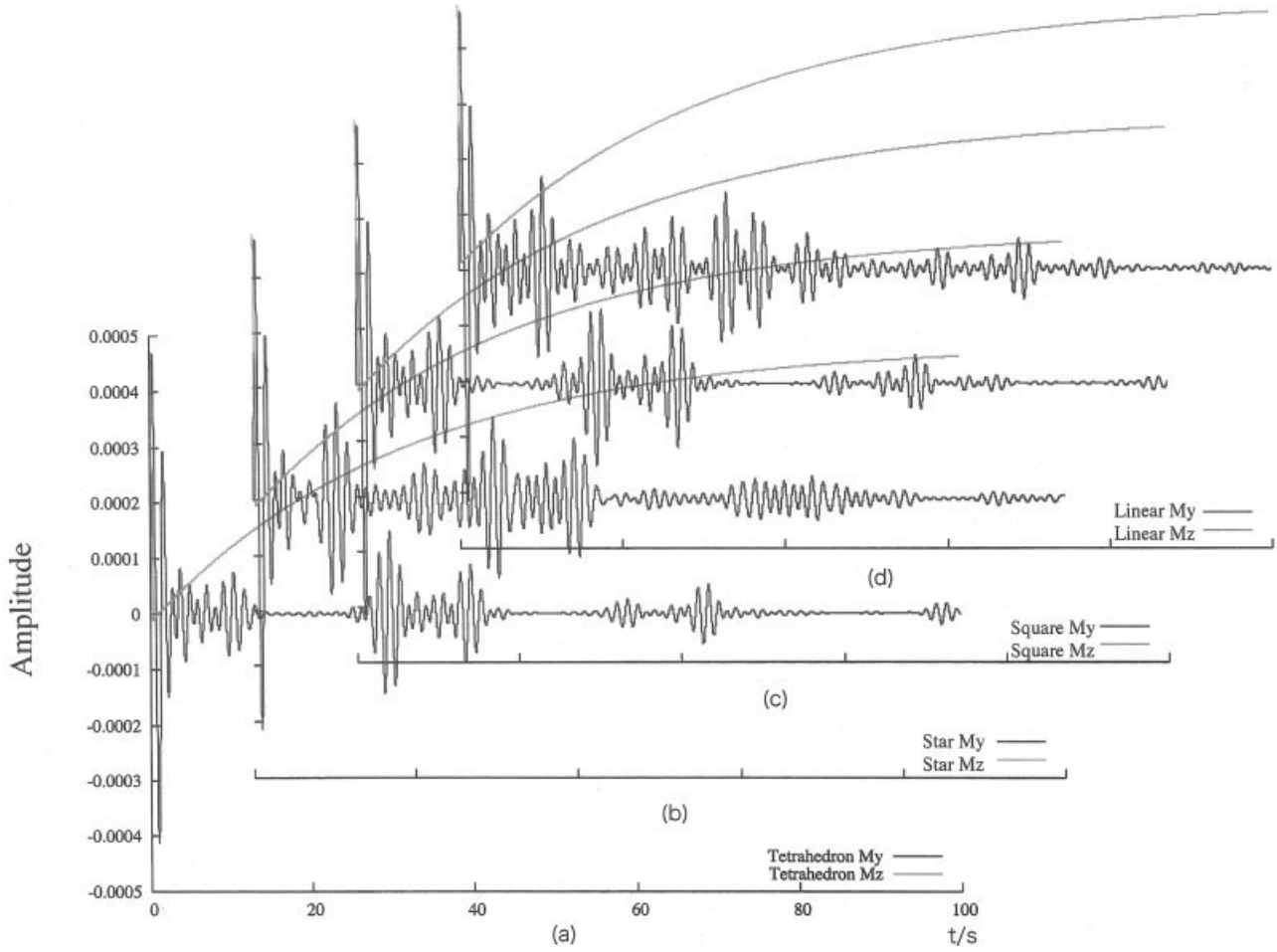

FIGURE 8. Variation of spin population (*Mz*) and coherency (*My*) for tetrahedron type (a), star type (b), square type (c), and linear type (d).

posed by Leuenberger and Loss [44]. Figure 7(b) shows the paths of population migration among spin states in both weak (left) and strong (right) cases. These paths correspond to the transitions with the change of one quantum spin number, caused by the action of $S+$ and $S-$. In the case of $J < B$, there are four paths. In contrast, in the case of $J > B$, there are two paths, which have same excitation–energy differences because of strong magnetic interactions.

4.2. FOUR-SPIN SYSTEMS

Figure 5(b) shows four types of four-spin systems (linear type, square type, star type, and tetrahedron type) that have magnetic interactions between neighboring spin sites, which is assumed to be weak coupling $J = 0.0005$ cm^{-1}. To distinguish among four sites, g value is assumed to be $g1 = 0.9$, $g2 = 0.8$, $g3 = 0.7$, and $g4 = 0.6$ in all structures. The relaxation parameter is fixed at $C = 0.005$. These spin models are modeled after the ferromagnetic compounds. In initial equilibrium, the ground state has $S = 2$ and their spontaneous magnetization (0.00064 for the linear-type system) is almost 6 times as that of the two spin model (0.00011). Figure 8 shows the spin dynamics for each spin system. As seen from the results of the *Mz* values, the aspects of population relaxations are found to be similar to each other because such dynamics depend on the energy level originating in the Zeeman splitting. As seen from the results of the *My* values, the aspects of the phase relaxation in four systems are found to be different from each other. The changes in the phase relaxations are determined by spin states, related to the structures of spin systems. This result

indicates the possibility for the control of the phase relaxation by the structure of the spin clusters.

5. Concluding Remarks

5.1. SUMMARY

We have performed spin dynamics in electron–spin systems using the quantum Liouville equation with the relaxation processes between spin states. For the two-spin system, we consider the two cases; one is the strong-coupling case, and the other is the weak one. The differences in population relaxation are not observed because population relaxation depends on the Zeeman splitting by external static magnetic field or the g factor at spin site. In contrast, the intensity of the coupling changes the aspects of the phase relaxation because the coupling between spins determines the spin states constructed by the diagonaling the spin Hamiltonian.

For four-spin systems, we examine the spin dynamics varying the structures of the spin system. The aspects of population relaxations are found to be similar to each other because such dynamics depend on the energy level that originates in the Zeeman splitting mentioned above. However, the aspects of the phase relaxation in four systems are found to be different from each other. The changes in phase relaxation are determined by spin states, related by the structures of spin systems. This result indicates the possibility for the control of the phase relaxation by the structure of the spin clusters.

5.2. QUANTUM COMPUTING

In a previous report [39], we have discussed the superposed and entangled states of quantum systems. The spin–boson model has been employed for a unified description of quantum electron (nuclear) spins, exciton, quantum light, Bose–Einstein condensation (BEC), BCS superconductor, and so forth, as illustrated in Figure 9. One of the required conditions [42, 43] for quantum computing by the use of these systems is that the coherence time should be longer than the gating time. Rabi oscillation of exciton has been found in the semiconductor quantum device, but the coherence time is only pico second [84]. The quantum beat of exciton has been observed even for π-electron system by the ultrafast spectroscopy [85]. In contrast, it is very long (10^3 s, even at room temperature) for nuclear spin [86]. In fact, the quantum computing was realized by using

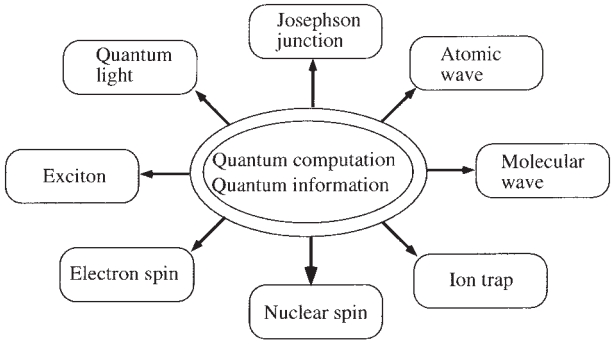

FIGURE 9. Spin–boson models for quantum systems.

seven nuclear spins [86]. Fortunately, the coherence time of electron spin in the semiconductor is found to be in microseconds [87]. This is similar to that of the Cooper pair box of superconductor [88]. The long coherence time might be accomplished in the case of molecular magnets by suppressing the hyperfine and other spin–boson (bath) interactions discussed in Section 2. This study is a first theoretical step for the rational design of molecular and cluster structures for elongation of their coherence time. The entanglement problem relating to quantum information transfer will be discussed elsewhere.

ACKNOWLEDGMENTS

M. T. is grateful for the financial support as Research Fellowships of the Japan Society for the Promotion of Science for Young Scientists and M. S. thanks for the financial support for the 21st Century COE program entitled the Creation of Integrated EcoChemistry at Osaka University.

References

1. Mitchell, P. Nature 1961, 191, 144.
2. Deisenhofer, J.; Epp, O.; Miki, K.; Huber, R.; Michel, H. Nature 1985, 318, 618.
3. McDermott, G.; Prince, S. M.; Freer, A. A.; Hawthornthwaite-Lawless, A. M.; Papiz, M. Z.; Cogdell, R. J.; Isaacs, N. W. Nature 1995, 374, 517.
4. Tsukihara, T.; Aotama, H.; Yamashita, E.; Tomizaki, T.; Yamaguchi, H.; Shinzawa-Itoh, K.; Nakashima, R.; Yaono, R.; Yoshikawa, S. Science 1995, 269, 1069.
5. Stryer, L. Biochemistry; 4th Ed.; W. H. Freeman: New York, 1995.
6. Tomalia, D. A.; Naylor, A. M.; Goddard, W. A., III. Angew Chem Int Ed 1990, 29, 138.

7. Takahata, M.; Nakano, M.; Fujita, H.; Yamaguchi, K. Chem Phys Lett 2002, 363, 422.
8. Takahata, M.; Nakano, M.; Yamaguchi, K.; J Theor Comp Chem 2003, 2, 459.
9. Nakano, M.; Takahata, M.; Fujita, H.; Kiribayashi, S.; Yamaguchi, K. Chem Phys Lett 2000, 323, 249.
10. Takahata, M.; Shoji, M.; Yamanaka, S.; Nakano, M.; Yamaguchi, K. Polyhedron 2005 (in press).
11. Kofman, A. G. Phys Rev A 2001, 64, 033809.
12. Gatteschi, D.; Yamaguchi, K. In Molecular Magnetism: From Molecular Assemblies to the Devices; Coronado, E.; Delhais, P.; Gatteschi, D.; Miller, J. S., Eds.; NATO, AS I series E, Vol. 321; Kluwer Academic Publishers: Dordrecht, 1996; p 561.
13. Yamaguchi, K. In Hyper-Structured Molecule; Vol. I: Chemistry, Physics and Applications; Sasabe, H., Ed.; Gordon & Breach Scientific: Japan, 1997; p 75.
14. Ito, K.; Kinoshita, M. Molecular Magnetism; Kodansha–Gordon & Breach: New York, 2000.
15. Sessoli, R.; Gatteschi, D.; Canesch, A.; Novak, M. A. Nature 1993, 365, 141.
16. Friedman, J. R.; Sarachik, M. P.; Tejada, J.; Ziolo, R. Phys Rev Lett 1996, 76, 3830.
17. Thomas, L.; Lionti, R.; Ballou, D.; Gatteschi, D.; Sessoli, R.; Barbara, B. Nature 1996, 383, 141.
18. Aubin, S. M. J.; Dilley, N. R.; Pardi, L.; Krzystek, J.; Wemple, M. W.; Brunel, L.-C.; Maple, M. B.; Christou, G.; Hendrickson, D. N. J Am Chem Soc 1998, 120, 4991.
19. Yang, E. C.; Hendrickson, D. N.; Wernsdorfer, W.; Nakano, M.; Zakharov, L. N.; Sommer, R. D.; Rheingold, A. L.; Ledezma-Gairaud, M.; Chirstou, G. J Appl Phys 2002, 91, 7382.
20. Oshio, H.; Hoshino, N.; Ito, T.; Nakano, M. J Am Chem Soc 2004, 126, 8805.
21. Douglass, D. C.; Cox, A. J.; Bucher, J. P.; Bloomfield, L. A. Phys Rev B 1993, 47, 12881.
22. Apsel, S. E.; Emmert, J. W.; Deng, J.; Bloomfield, L. A. Phys Rev Lett 1996, 76, 1442.
23. Hirt, A.; Gerion, D.; Billas, I. M. L.; Châtelain, A.; de Heer, W. A. Z Phys D 1997, 40, 160.
24. Glauber, J Math Phys 1963, 4, 294.
25. Heims, S. P. Phys Rev 1965, 138, A587.
26. Rey, T.; Ray, D. K. Phys Rev 1967, 164, 164.
27. Rikvold, P. A.; Tomita, H.; Miyashita, S.; Sidees, S. W. Phys Rev E 1994, 49, 5080.
28. De Raedt, H.; Miyashita, S.; Michielseu, K.; Machida, M. Phys Rev B 2004, 70, 064401.
29. Saakiam, D.; Hu, C.-K. Phys Rev E 2004, 69, 021913.
30. Caneschi, A.; Gatteschi, D.; Lailoti, N.; Sangregorio, C.; Sessoli, R.; Venturi, G.; Vindigni, A.; Rettori, A.; Pini, M. G.; Novak, M. A. Angew Chem Int Ed 2001, 40, 1760.
31. Clérac, R.; Miyasaka, H.; Yamashita, M.; Coulon, C. J Am Chem Soc 2002, 124, 12837.
32. Coulon, C.; Clerac, R.; Lecren, L.; Wernsdorfer, W.; Miyasaki, H. Phys Rev B 2004, 69, 132408.
33. Ferbinteanu, M.; Miyasaka, H.; Wernsdorfer, W.; Nakata, K.; Sugiura, K.-i.; Yamashita, M.; Coulon, C.; Clerac, R. J Am Chem Soc 2005, 127, 3090.
34. Yamaguchi, K.; Takahara, Y.; Fueno, T. In Applied Quantum Chemistry; Smith, V. H., Jr.; Schaefer, H. F., III; Morokuma, K.; Reidel, S. Kluwer Academic Publishers: Dordrecht 1986; p 155.
35. Yamanaka, S.; Okumura, M.; Nakano, M.; Yamaguchi, K. J Mol Struct (Theochem) 1994, 310, 205.
36. Takeda, R.; Mitsuo, S.; Yamanaka, S.; Yamaguchi, K. Polyhedron 2005 (in press).
37. Cox, A. J.; Louderback, J. G.; Bloomfield, L. A. Phys Rev Lett 1993, 71, 923.
38. Cox, A. J.; Louderback, J. G.; Apsel, S. E.; Bloomfield, L. A. Phys Rev B 1994, 49, 12295.
39. Yamaguchi, K.; Nakano, M.; Nagao, H.; Okumura, M.; Yamanaka, S.; Kawakami, T.; Yamaki, D.; Nishino, M.; Shigeta, Y.; Kitagawa, Y.; Takano, Y.; Takahata, M.; Takeda, R. Bull Korean Chem Soc 2003, 24, 864.
40. Yamanaka, S.; Yamaguchi, K. Bull Chem Soc Jpn 2004, 77, 1269.
41. Weiss, U. Quantum Dissipative Systems; World Scientific: Singapore, 1999.
42. Loss, D.; Di Vincenzo, D. P. Phys Rev A 1998, 57, 120.
43. Di Vincenzo, D. P.; Bacon, D.; Kempe, J.; Burkand, G.; Whaley, K. B. Nature 2000, 408, 339.
44. Leuenberger, M. N.; Loss, D. Nature 2001, 410, 789.
45. Imamoglu, A.; Awschalom, D. D.; Burkard, G.; DiVincenzo, D. P.; Loss, D.; Sherwin, M.; Small, A. Phys Rev Lett 1999, 83, 4204.
46. Nakano, M.; Fujita, H.; Takahata, M.; Yamaguchi, K. J Chem Phys 2001, 115, 1052.
47. Natano, M.; Takahata, M.; Yamada, S.; Yamaguchi, K.; Kishi, R.; Nitta, T. J Chem Phys 2004, 120, 2359.
48. Nakano, M.; Yamaguchi, K. Phys Rev A 1994, 50, 2989.
49. Yamaguchi, K.; Yamanaka, S.; Nishino, M.; Takano, Y.; Kitagawa, Y.; Nagao, H.; Yoshioka, Y. Theor Chem Acc 1999, 102, 328.
50. Cheche, T. O.; Lin, S. H. Phys Rev E 2001, 64, 061103.
51. Stamp, P. C. E.; Tupitsyn, I. S. Chem Phys 2004, 296, 281.
52. Vorrath, T.; Brandas, T.; Kramer, B. Chem Phys 2004, 296, 295.
53. Paladino, E.; Sassetti, M.; Falci, G. Chem Phys 2004, 296, 325.
54. Thorwart, M.; Paladino, E.; Grifori, M. Chem Phys 2004, 296, 333.
55. Wilhelm, F. K.; Kleff, S.; von Delft, J. Chem Phys 2004, 296, 345.
56. Nagao, H.; Yamanaka, S.; Nishino, M.; Yoshioka, Y.; Yamaguchi, K. Chem Phys Lett 1999, 302, 418.
57. Nagao, H.; Nishino, M.; Shigeta, Y.; Soda, T.; Kitagawa, Y.; Onishi, T.; Yoshioka, Y.; Yamaguchi, K. Coord Chem Rev 2000, 198, 265.
58. Nishino, M.; Yamaguchi, K.; Miyashita, S. Phys Rev B 1998, 58, 9303.
59. Nishino, M.; Nagao, H.; Yoshioka, Y.; Yamaguchi, K. Mol Crystallogr Liq Crystallogr 1999, 335, 593.
60. Shigeta, Y.; Kawakami, T.; Nagao, H.; Yamaguchi, K. Chem Phys Lett 1999, 315, 441.
61. Lascialfari, A.; Gatteschi, D.; Cornia, A.; Balucani, U.; Pini, M. G.; Rettori, A. Phys Rev B 1998, 57, 1115.

62. Garanin, D. A.; Chudnovsky, E. M.; Schilling, R. S. Phys Rev B 2000, 61, 12204.
63. Lascialfari, A.; Jang, Z. H.; Borsa, F.; Gatteschi, D.; Cornia, A.; Rovai, D.; Caneschi, A.; Carretta, P. Phys Rev B 2000, 61, 6839.
64. Caneschi, A.; Cornia, A.; Fabretti, A. C.; Foner, S.; Gatteschi, D.; Grandi, R.; Schenetti, L. Chem Eur J 1996, 2, 1379.
65. Lascialfari, A.; Gatteschi, D.; Borsa, F.; Cornia, A. Phys Rev B 1997, 55, 14341.
66. Gütlich, P.; Hauzer, A.; Spiering, H. Angew Chem Int Ed 1994, 33, 2024.
67. Chiorescu, I.; Giraud, R.; Jansen, A. G. M.; Caneschi, A.; Barbara, B. Phys Rev Lett 2000, 85, 4807.
68. Pohjola, T.; Schoeller, H. Phys Rev B 2000, 62, 15026.
69. Leuenberger, M. N.; Loww, D. Phys Rev B 2000, 61, 1286.
70. Jakob, M.; Stenholm, S. Phys Rev A 2004, 70, 012104.
71. Wernsdorfer, W. Adv Chem Phys 2001, 118, 99.
72. Shoji, M.; Koizumi, K.; Hamamoto, T.; Taniguchi, T.; Takeda, R.; Kitagawa, Y.; Kawakami, T.; Okumura, M.; Yamanaka, S.; Yamaguchi, K. Polyhedron 2005 (in press).
73. Takeda, R.; Yamanaka, S.; Yamaguchi, K. Int J Quantum Chem 2005, 102, 80.
74. Barra, A. L.; Gatteschi, D.; Sessoli, R. Phys Rev B 1997, 56, 8192.
75. Kitagawa, M.; Ueda, M. Phys Rev A 1993, 47, 5138.
76. Nakajima, T.; Aoki, H. Phys Rev B 1997, 56, 1215549.
77. Sprensen, A.; Mlmer, K. Phys Rev Lett 1999, 83, 2274.
78. Jakob, M.; Stenholm, S. Phys Rev A 2004, 70, 012104.
79. Manassen, Y.; Ovanesyan, E. T.; Shachal, D.; Richter, S. Phys Rev B 1993, 48, 4887.
80. Hammel, P. C. Nature 2004, 430, 300.
81. Rugar, D.; Budakian, R.; Mamin, H. J.; Chui, B. W. Nature 2004, 430, 329.
82. Elzerman, J. M.; Hanson, R.; Willems van Beveren, L. H.; Witkamp, B.; Vandersypen, L. M. K.; Kouwenhoven, L. P. Nature 2004, 430, 431.
83. Twamley, J. Phys Rev A 2003, 67, 052318.
84. Kamada, K.; Gotoh, H.; Temmyo, J.; Takagahara, T.; Ando, H. Phys Rev Lett 2001, 87, 246401.
85. Yamazaki, I.; Akimoto, S.; Yamazaki, T.; Saito, S.-i.; Sakata, Y. J Phys Chem A 2002, 106, 2122.
86. Vandersypen, L. M. K.; Steffen, M.; Breyta, G.; Yannoni, C. S.; Sherwood, M. H.; Chuang, I. L. Nature 2001, 414, 883.
87. Kikkawa, J. M.; Smorchkova, I. P.; Samarth, N.; Awschalom, D. D. Science 1997, 277, 1284.
88. Vin, D.; Aassime, A.; Cottet, A.; Joyez, P.; Pothier, H.; Urbina, C.; Esteve, D.; Devoret, M. H. Science 2002, 296, 886.